doi:10.1093/brain/awt142 Brain 2013: 136; 2217–2227 | 2217

BRAIN
A JOURNAL OF NEUROLOGY

Amyloid tracers detect multiple binding sites in Alzheimer's disease brain tissue

Ruiqing Ni,[1] Per-Göran Gillberg,[1] Assar Bergfors,[1] Amelia Marutle[1] and Agneta Nordberg[1,2]

1 Alzheimer Neurobiology Centre, Department of Neurobiology, Care Sciences and Society, Karolinska Institutet, Stockholm, Sweden
2 Department of Geriatric Medicine, Karolinska University Hospital Huddinge, S-141 86 Stockholm, Sweden

Correspondence to: Professor Agneta Nordberg, MD, PhD,
Karolinska Institutet, Department of Neurobiology,
Care Sciences and Society,
Alzheimer Neurobiology Center,
Karolinska University Hospital Huddinge,
Novum 5th Floor, S-14186 Stockholm,
Sweden
E-mail: Agneta.K.Nordberg@ki.se

Imaging fibrillar amyloid-β deposition in the human brain *in vivo* by positron emission tomography has improved our understanding of the time course of amyloid-β pathology in Alzheimer's disease. The most widely used amyloid-β imaging tracer so far is ^{11}C-Pittsburgh compound B, a thioflavin derivative but other ^{11}C- and ^{18}F-labelled amyloid-β tracers have been studied in patients with Alzheimer's disease and cognitively normal control subjects. However, it has not yet been established whether different amyloid tracers bind to identical sites on amyloid-β fibrils, offering the same ability to detect the regional amyloid-β burden in the brains. In this study, we characterized ^{3}H-Pittsburgh compound B binding in autopsied brain regions from 23 patients with Alzheimer's disease and 20 control subjects (aged 50 to 88 years). The binding properties of the amyloid tracers FDDNP, AV-45, AV-1 and BF-227 were also compared with those of ^{3}H-Pittsburgh compound B in the frontal cortices of patients with Alzheimer's disease. Saturation binding studies revealed the presence of high- and low-affinity ^{3}H-Pittsburgh compound B binding sites in the frontal cortex (K_{d1}: 3.5 ± 1.6 nM; K_{d2}: 133 ± 30 nM) and hippocampus (K_{d1}:5.6 ± 2.2 nM; K_{d2}: 181 ± 132 nM) of Alzheimer's disease brains. The relative proportion of high-affinity to low-affinity sites was 6:1 in the frontal cortex and 3:1 in the hippocampus. One control showed both high- and low-affinity ^{3}H-Pittsburgh compound B binding sites (K_{d1}: 1.6 nM; K_{d2}: 330 nM) in the cortex while the others only had a low-affinity site (K_{d2}: 191 ± 70 nM). ^{3}H-Pittsburgh compound B binding in Alzheimer's disease brains was higher in the frontal and parietal cortices than in the caudate nucleus and hippocampus, and negligible in the cerebellum. Competitive binding studies with ^{3}H-Pittsburgh compound B in the frontal cortices of Alzheimer's disease brains revealed high- and low-affinity binding sites for BTA-1 (K_i: 0.2 nM, 70 nM), florbetapir (1.8 nM, 53 nM) and florbetaben (1.0 nM, 65 nM). BF-227 displaced 83% of ^{3}H-Pittsburgh compound B binding, mainly at a low-affinity site (311 nM), whereas FDDNP only partly displaced (40%). We propose a multiple binding site model for the amyloid tracers (binding sites 1, 2 and 3), where AV-45 (florbetapir), AV-1 (florbetaben), and Pittsburgh compound B, all show nanomolar affinity for the high-affinity site (binding site 1), as visualized by positron emission tomography. BF-227 shows mainly binding to site 3 and FDDNP shows only some binding to site 2. Different amyloid tracers may provide new insight into the pathophysiological mechanisms in the progression of Alzheimer's disease.

Keywords: Alzheimer's disease; β-amyloid imaging ligands; β-amyloid fibril binding sites; PIB; post-mortem brain

Abbreviation: PIB = Pittsburgh compound B

Received November 24, 2012. Revised April 4, 2013. Accepted April 10, 2013. Advance Access publication June 11, 2013

Introduction

Alzheimer's disease is the most common neurodegenerative disorder. The accumulation of amyloid-β in the brain is one of the earliest pathological hallmarks of the disease and is considered to play a key role in Alzheimer's disease pathogenesis. Recent developments in molecular imaging have made it possible to visualize the fibrillar amyloid-β plaques in the brains of living patients with Alzheimer's disease, using PET (Nordberg *et al*., 2010; Reiman and Jagust, 2012). New criteria for the early diagnosis of Alzheimer's disease suggest the combined use of PET amyloid imaging and CSF biomarkers (Dubois *et al*., 2010; McKhann *et al*., 2011, Sperling *et al*., 2011).

^{11}C-Pittsburgh compound B (PIB) is a widely studied amyloid tracer that detects fibrillar amyloid-β with high accuracy (Klunk *et al*., 2004; Nordberg *et al*., 2010; Rowe and Villemagne, 2011). PET has demonstrated high PIB retention in cortical brain regions of patients with Alzheimer's disease (Klunk *et al*., 2004; Engler *et al*., 2006; Rowe *et al*., 2010) and patients with mild cognitive impairment that later converted to Alzheimer's disease (Kemppainen *et al*., 2007; Forsberg *et al*., 2008; Jack *et al*., 2009; Nordberg *et al*., 2013). Moreover, 10–30% of cognitively normal adults demonstrate a high presence of amyloid-β plaques in the brain according to ^{11}C-PIB measurements, and the prevalence increases with age (Mintun *et al*., 2006; Pike *et al*., 2007; Rowe *et al*., 2007; Aizenstein *et al*., 2008; Morris *et al*., 2010; Villemagne *et al*., 2011, 2013; Nordberg *et al*., 2013). However, although amyloid PET imaging has contributed to a better understanding of amyloid-β processes *in vivo*, the molecular mechanisms and binding properties of amyloid tracers in the brains of patients with Alzheimer's disease and cognitively normal adults are not yet fully understood.

The amyloid PET tracers developed to date belong to various chemical classes, including thioflavin T (^{11}C-PIB, Klunk *et al*., 2004; ^{18}F-flutemetamol, Nelissen *et al*., 2009; ^{11}C-AZD2184, Nyberg *et al*., 2009), stilbenes (^{18}F-AV-45, Clark *et al*., 2011; ^{18}F-AV-1, Rowe *et al*., 2008; and ^{11}C-SB-13, Verhoeff *et al*., 2004), benzoxazoles (^{11}C-BF-227, Kudo *et al*., 2007; ^{18}F-BF-227, Harada *et al*., 2013), aminonaphthalenes (^{18}F-FDDNP, Shoghi-Jadid *et al*., 2002) and benzofurans (^{18}F-AZD4694, Cselenyi *et al*., 2012). The fact that different amyloid PET tracers emanate from different chemical classes may suggest that in addition to similarities, they may also show dissimilarities in binding properties to fibrillar amyloid-β and also bind to other forms of amyloid-βs. The extent of possible differences between different amyloid tracers in binding profiles and detection of fibrillar amyloid-β deposits in the Alzheimer's disease brain has not been thoroughly investigated.

Several ^{18}F-labelled amyloid tracers have been developed and evaluated in clinical studies. These include ^{18}F-FDDNP (Shoghi-Jadid *et al*., 2002), ^{18}F-AV-45 (^{18}F-florbetapir, Wong *et al*., 2010; Clark *et al*., 2011), ^{18}F-AV-1 (^{18}F-florbetaben, Rowe *et al*., 2008; Barthel *et al*., 2011), ^{18}F-flutemetamol (Vandenberghe *et al*., 2010) and ^{18}F-AZD4694 (Cselenyi *et al*., 2012). Recent head to head comparison studies suggested a strong association of cortical retention between ^{11}C-PIB and ^{18}F-florbetapir (Landau *et al*., 2013), ^{18}F-florbetaben (Villemagne *et al*., 2012*b*, Wolk *et al*., 2012) and ^{18}F-flutemetamol (Vandenberghe *et al*., 2010).

Owing to the short 20-min half-life of ^{11}C-compounds, the use of ^{11}C- is limited to research hospitals that are equipped with an on-site cyclotron. The development of ^{18}F-labelled amyloid tracers with >5-fold longer half-life provides the possibility of transportation of the radiotracer from a cyclotron unit to hospitals at some distance. The ^{18}F-labelled amyloid tracers will thereby be more suitable for clinical use. In addition, the 10-min scan period used with the ^{18}F tracers, instead of the 60–90 min scanning with ^{11}C-amyloid tracers offers wider application in clinical settings. ^{18}F-florbetapir was approved by the Food and Drug Administration (FDA) in 2012 and by the European Medicines Agency (EMA) in 2013 for clinical assessment of memory disorders. A report on appropriate use criteria for amyloid PET has recently been published (Johnson *et al*., 2013).

In vivo PET evidence of ^{11}C-PIB retention strongly correlates with quantitatively measured amyloid-β levels in Alzheimer's disease brains at autopsy (Ikonomovic *et al*., 2008; Kadir *et al*., 2011). Similarly, a close relationship between *in vivo* amyloid tracer retention and histopathological assessment of amyloid pathology has been reported in brain biopsies for ^{11}C-PIB, ^{18}F-flutemetamol (Leinonen *et al*., 2008, 2013) and at autopsy for ^{11}C-PIB (Driscoll *et al*., 2012), (^{18}F-florbetapir) (Clark *et al*., 2011, 2012), 18F-AV-1 (^{18}F-flutemetamol) (Wolk *et al*., 2011).

The aim of this study was to characterize the regional ^{3}H-PIB binding properties in Alzheimer's disease and cognitively normal control post-mortem brain tissues and to compare the corresponding detection of fibrillar amyloid-β pathology with that of amyloid PET tracers BTA-1, AV-1, AV-45, BF-227 and FDDNP in Alzheimer's disease brain tissue.

Material and methods

Tracers

[*N*-methyl-^{3}H]2-(4′-methylaminophenyl)-6-hydroxybenzothiazole (^{3}H-PIB, specific activity 68–85 Ci/mmol) was custom synthesized by GE Healthcare. Benzenamine 4-[(1E)-2-[6-[2-[2-(2-fluoroethoxy)ethoxy]ethoxy]-3-pyridinyl]ethenyl]-*N*-methyl (AV-45), and benzenamine 4-[(1E)-2-[4-[2-[2-(2-fluoroethoxy)ethoxy]ethoxy]phenyl]ethenyl]-*N*-methyl (AV-1) were kind gifts from Dr Ian M. Newington (GE Healthcare). 2-(4′-Methylaminophenyl) benzothiazole (BTA-1) was purchased from Sigma Aldrich. 2-(1-(6-[(2-fluoroethyl-(methyl)amino]-2-naphthyl)ethylidene) malononitrile (FDDNP) was a kind gift from Dr Jorge R. Barrio (UCLA, USA) and 2-(2-[2-dimethylaminothiazol-5-yl]ethenyl)-6-(2-[fluoro]ethoxy) benzoxazole (BF-227) was a kind gift from Dr Nobuyuki Okamura (Department of Pharmacology, Tohoku University School of Medicine, Sendai, Japan).

Alzheimer's disease versus control brain studies

Brain tissue from 23 patients with Alzheimer's disease (mean age 70.5 ± 9.0 years; mean post-mortem delay 6.1 ± 2.9 h), clinically

diagnosed and confirmed by pathological examination according to NINCDS-ADRDA criteria, and 20 age-matched cognitively normal control subjects (mean age 73.8 ± 11.6 years; mean post-mortem delay 9.2 ± 6.0 h) was obtained at autopsy and provided by the Huddinge Brain Bank, Karolinska University Hospital Huddinge, Sweden, and the Netherlands Brain Bank, Netherlands Institute for Brain Research (Table 1). Thirteen of the patients with Alzheimer's disease had been clinically diagnosed with early-onset Alzheimer's disease before reaching 65 years of age (mean age 63.9 ± 5.0 years; mean post-mortem delay 5.9 ± 3.4 h). The other 10 patients were diagnosed after 65 years of age with late-onset Alzheimer's disease (mean age 79.1 ± 4.6 years; mean post-mortem delay 6.2 ± 0.4 h). Detailed demographic information is presented in Table 1. Permission to use autopsy brain material in experimental procedures was granted by the Regional Human Ethics committee in Stockholm and the Swedish Ministry of Health.

Apolipoprotein E genotyping

Genomic DNA was extracted from frozen brain tissues using a QIAamp® DNA mini kit (Qiagen). The apolipoprotein E (*APOE*) genotype was determined using an INNO-LiPA ApoE kit (Innogenetics) according to the manufacturer's instructions.

Homogenate tissue preparation

Frozen post-mortem tissue samples obtained from the superior frontal gyri, superior parietal gyri, hippocampi, caudate nuclei and cerebella of 23 Alzheimer's disease and 20 control brains were homogenized in cold 0.32 M sucrose buffer containing phosphatase and protease inhibitors. The homogenates were aliquoted and stored at −80°C until use in binding experiments.

^{3}H-Pittsburgh compound B binding assays

^{3}H-PIB was chosen for the *in vitro* binding experiments due to the stable properties and long-half-life of ^{3}H-compounds. In the ^{3}H-PIB binding assays, brain homogenates were incubated with 1 nM ^{3}H-PIB (specific activity 85 Ci/mmol) for 2 h at room temperature in agreement with the filtration assay in Kadir *et al.* (2011). Specific binding was expressed in pmol/g tissue, and non-specific binding was determined in the presence of 1 μM BTA-1. Saturation binding assays were performed by incubating ^{3}H-PIB (0.1 nM to 300 nM) with frontal cortex and hippocampus homogenates (50 μg tissue) from five Alzheimer's disease and five control brains. Competition binding assays were carried out by incubating frontal cortex homogenates (50 μg tissue) from five Alzheimer's disease brains with 1 nM ^{3}H-PIB and in the presence of BTA-1, AV-45, AV-1, BF-227 and FDDNP at concentrations ranging from 10^{-13} to 5×10^{-6} M. The dissociation constant (K_d), maximum number of binding sites (B_{max}), affinity constant (K_i) and percentage of displacement in the saturation and displacement analyses were determined by using non-linear regression models in GraphPad Prism version 5.0 (GraphPad Software, Inc.). The saturation data were fit to the equation

Table 1 Demographic information for Alzheimer's disease and control brains

	AD	Control
Number of brains:	23	20
Age (years, range)	70.5 ± 9.0 (58–87)	73.8 ± 11.6 (50–88)
Sex (female/male)	13/10	9/11
APOE ε4 (0/1/2)	7/7/9	20/0/0
Alzheimer's disease duration (years)	6.6 ± 2.5	-
Post-mortem delay (h)	6.1 ± 2.9	9.2 ± 6.0
Braak stage (range)	5.1 ± 0.7 (4–6)	1.6 ± 0.6 (1–3)

0/1/2 = number of alleles. Data are shown as mean ± standard deviation.

$Y = B_{max}*X / (K_d + X)$ for one-site binding model; and $Y = [B_{max1}*X / (K_{d1} + X)] + [B_{max2}*X / (K_{d2} + X)]$ for two-site binding model. The displacement results were fit to one-site and two-site binding models derived from the Cheng-Prusoff equation. F-test was used to compare and select the one-site or two-site binding models. Scatchard plots were performed using GraphPad Prism to display the saturation data.

Total amyloid-β_{40} and amyloid-β_{42} measurement

Total amyloid-β_{40} and amyloid-β_{42} level were quantified in the post-mortem brain tissue from the frontal cortex and hippocampus of five Alzheimer's disease and five control using commercial ELISA kits (Invitrogen).

Statistical analysis

Data were analysed using GraphPad Prism version 5.0. The non-parametric Mann-Whitney U test was used for comparison of ^{3}H-PIB binding properties, amyloid-β_{40} and amyloid-β_{42} levels, between Alzheimer's disease and control brains, and the paired Student *t*-test was used for comparison between brain regions. All values are shown as means ± standard deviation. Error bars in the figures represent standard error values.

Results

Characterization of ^{3}H-Pittsburgh compound B binding sites in Alzheimer's disease frontal cortex and hippocampus

To examine the high-affinity ^{3}H-PIB binding sites in the brain, saturation binding studies using increasing concentrations of ^{3}H-PIB (0.01–30 nM) were performed *in vitro* on post-mortem tissue from the frontal cortex and hippocampus of five patients with Alzheimer's disease (aged 61–87 years). Figure 1 illustrates saturation binding in three of these patients (aged 61, 68 and 87 years). Scatchard plots demonstrated high-affinity binding sites in the frontal cortices (mean K_{d1}: 3.5 ± 1.6 nM) and the

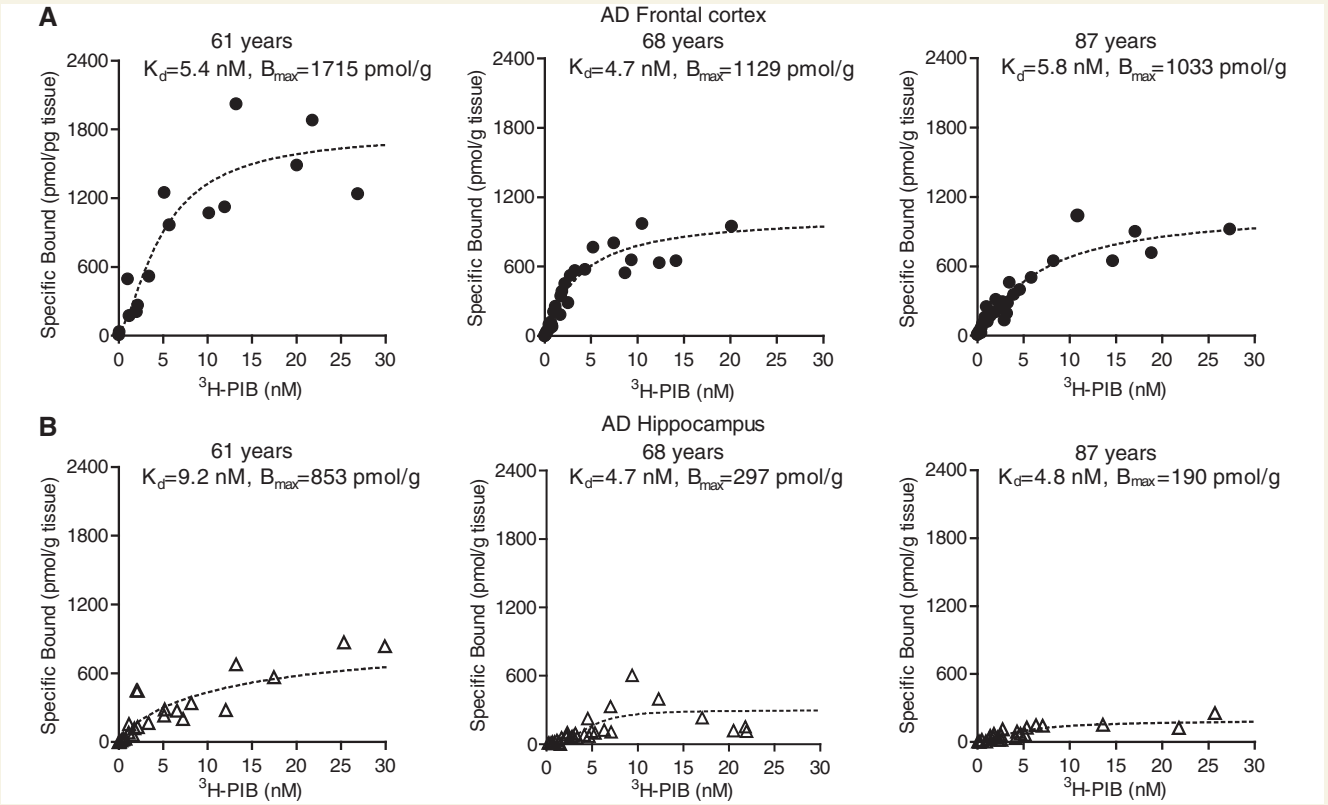

Figure 1 Saturation binding of ^{3}H-PIB (0.01–30 nM) indicated a high-affinity binding site in the frontal cortices (**A**) and hippocampi (**B**) of brains from patients with Alzheimer's disease (AD) (61 years; 68 years; 87 years). Binding data were analysed using GraphPad non-linear regression fitting.

hippocampi (mean K_{d1}: 5.6 ± 2.2 nM) of all five, with a significantly ($P < 0.01$) greater number of ^{3}H-PIB high-affinity binding sites in the frontal cortex (mean B_{max1}: 1281 ± 423 pmol/g tissue) than in the hippocampus (mean B_{max1}: 530 ± 277 pmol/g tissue) (Table 2). Analysis of total amyloid-β_{40} and amyloid-β_{42} levels quantified by ELISA revealed significant higher amyloid-β levels in the frontal cortex compared with hippocampus ($P < 0.05$) (Table 3). ^{3}H-PIB binding performed in the same brain tissue samples as the amyloid-β ELISA measurements showed a 5-fold difference in ^{3}H-PIB binding whereas a 10-fold difference in amyloid-β_{40+42} levels in the frontal cortex compared with hippocampus (Table 3) was detected by ELISA. The amyloid-β_{40}, amyloid-β_{42} and amyloid-β_{40+42} levels all showed a significant positive correlation with ^{3}H-PIB binding (1 nM) ($P < 0.05$) in the corresponding brain region.

To further characterize ^{3}H-PIB binding sites in the Alzheimer's disease brain, homogenates from the frontal cortices and hippocampi of five Alzheimer's disease brains were incubated with a wider range of ^{3}H-PIB concentrations (0.01–300 nM; Table 2). Supplementary Fig. 1 shows the saturation binding curve (0.01–300 nM) in the frontal cortex of one Alzheimer's disease brain (78 years). In addition to the high-affinity site described above, the Scatchard plots revealed the presence of low-affinity ^{3}H-PIB binding sites in the frontal cortices (mean K_{d2}: 133 ± 30 nM) and the hippocampi (mean K_{d2}: 181 ± 132 nM) of the five Alzheimer's disease brains (Table 2). No significant differences in dissociation constants for the high- and low-affinity sites (K_{d1} and K_{d2}) were observed between the frontal cortex and the hippocampus (Table 2). The B_{max} value for the high-affinity site (B_{max1}), but not the low-affinity site (B_{max2}), in the frontal cortex was significantly higher than that in the hippocampus.

Characterization of ^{3}H-Pittsburgh compound B binding sites in control frontal cortex and hippocampus

Saturation binding studies with ^{3}H-PIB 0.1 to 300 nM were also performed in the frontal cortices and hippocampi of five control brains (from patients aged 54–87 years). Analysis revealed ^{3}H-PIB high-affinity binding (similar to that seen in the Alzheimer's disease frontal cortex; Supplementary Fig. 2A and B) in the frontal cortex of only one (87-year-old) control subject, with a K_{d1} of 1.6 nM and B_{max1} of 309 pmol/g. All three control brains tissues that incubated with wider range (0.1–300 nM) of ^{3}H-PIB showed evidence of a low-affinity site in the frontal cortex with comparable K_{d2} values (191 ± 70 nM) to those in Alzheimer's disease brains (133 ± 30 nM) (Supplementary Fig. 2C and D). In the hippocampus of the 87-year-old control subject, only a low-affinity binding site was detected (K_{d2}: 136 nM; B_{max2}: 2788 pmol/g). The presence of some amyloid-β_{42} plaques in the frontal cortex of this 87-year-old control brain was confirmed by

Table 2 ^{3}H-PIB binding properties in the frontal cortex and hippocampus of brains from patients with Alzheimer's disease

	Patient age (years)	K_{d1} nM	K_{d2} nM	B_{max1} (pmol/g tissue)	B_{max2} (pmol/g tissue)	% High	% Low	R^2
Frontal cortex	AD 61	4.8	219.5	1771	7393	91.3	8.7	0.9282
	AD 68	3.6	184.9	1022	4792	91.5	8.5	0.9656
	AD 70	2.5	81.7	1677	8120	87.1	12.9	0.8744
	AD 78	1.2	114.2	1137	17220	86.0	14.0	0.9840
	AD 87	5.2	65.5	799	3530	74.0	26.0	0.9203
	Mean ± SD	3.5 ± 1.6	133.2 ± 29.8	1281 ± 423**	8211 ± 2403	86.0 ± 3.2*	14.0 ± 3.2*	0.9345 ± 0.0191*
Hippocampus	AD 61	9.2	210.4	853	7451	72.4	27.6	0.6936
	AD 68	4.7	361.4	297	10774	67.8	32.2	0.9541
	AD 70	3.5	59.3	621	2486	80.8	19.2	0.7968
	AD 78	5.8	229.9	687	9074	75.0	25.0	0.7881
	AD 87	4.8	43.0	190	761.2	69.1	30.9	0.7429
	Mean ± SD	5.6 ± 2.2	180.8 ± 132.0	530 ± 277	6109 ± 4303	73.0 ± 5.2	27.0 ± 5.2	0.7951 ± 0.0979

B_{max1} and B_{max2} = maximum number of high- and low-affinity binding sites; % High = percentage of high-affinity binding sites; K_{d1} and K_{d2} = high- and low-affinity site dissociation constants; % Low = percentage of low-affinity binding sites; R^2 = extent of the fit to the nonlinear regression two-binding-site model; SD = standard deviation. Significant differences between frontal cortex and hippocampus (paired *t*-test; $n = 5$) are indicated by $^{*}P < 0.05$ and $^{**}P < 0.01$.

Table 3 Amyloid-β_{40} and amyloid-β_{42} levels in the frontal cortices and hippocampi and ^{3}H-PIB binding in Alzheimer's disease and control brains

	Amyloid-β_{40} (pmol/g tissue)	Amyloid-β_{42} (pmol/g tissue)	Amyloid-β_{40} + amyloid-β_{42} (pmol/g tissue)	^{3}H-PIB (1 nM) binding (pmol/g tissue)
Alzheimer's disease frontal cortex	613.70 ± 537.20**†	1328.00 ± 459.80**†	1941.00 ± 1913.00**†	524.63 ± 113.82**†
Alzheimer's disease hippocampus	26.50 ± 12.30*	140.70 ± 129.60*	167.10 ± 137.80*	89.71 ± 62.27*
Control frontal cortex	0.06 ± 0.02	0.17 ± 0.13	0.22 ± 0.15	73.89 ± 30.85
Control hippocampus	0.16 ± 0.23	0.09 ± 0.06	0.24 ± 0.34	19.10 ± 14.10

Data are shown as means ± standard deviation. Significant differences between frontal cortex and hippocampus are indicated by $^{\dagger}P < 0.05$. Significant differences between Alzheimer's disease ($n = 5$) and control ($n = 5$) groups (Mann-Whitney U-test) are indicated by $^{*}P < 0.05$, $^{**}P < 0.01$.

immunohistochemical staining (data not shown). Total amyloid-β_{40} and amyloid-β_{42} ELISA measurements showed low levels in the frontal cortex as well as in the hippocampus (Table 3).

Regional distribution of ^{3}H-Pittsburgh compound B binding in Alzheimer's disease and control brain tissue

The distribution of ^{3}H-PIB (1 nM) binding was studied in the frontal and parietal cortices, caudate nuclei, hippocampi and cerebella of 23 patients with Alzheimer's disease (mean age 70.5 ± 9.0 years) and 20 normal control subjects (mean age 73.8 ± 11.6 years). ^{3}H-PIB binding in Alzheimer's disease brains was highest in the frontal and parietal cortices, followed in order by the caudate nucleus, hippocampus and cerebellum (Fig. 2). ^{3}H-PIB binding was significantly higher in the frontal and parietal cortices ($P < 0.001$), hippocampi ($P < 0.01$) and caudate nuclei ($P < 0.001$) of Alzheimer's disease brains than in age-matched controls (Fig. 2). Although a significant difference in ^{3}H-PIB binding was observed between controls versus early-onset Alzheimer's disease and control versus late-onset Alzheimer's disease, no significant difference was found between early-onset and late-onset Alzheimer's disease (Fig. 2). No significant difference in binding was observed between Alzheimer's disease APOE $\varepsilon 4$ ($n = 16$) and non-$\varepsilon 4$ ($n = 7$) carriers (data not shown).

^{3}H-Pittsburgh compound B competitive binding assays with BTA-1, AV-45, AV-1, BF-227 and FDDNP in Alzheimer's disease frontal cortex

Displacement assays were carried out to compare the binding properties of various amyloid ligands in Alzheimer's disease brains. Increasing concentrations of unlabelled BTA-1, AV-45, AV-1, BF-227 and FDDNP (10^{-13}– 5×10^{-6} M) were applied with ^{3}H-PIB (1 nM) to frontal cortex homogenates from the same five Alzheimer's disease brains used in the binding characterization studies. BTA-1 was selected for displacement studies with ^{3}H-PIB in order to measure the displacement binding properties of PIB.

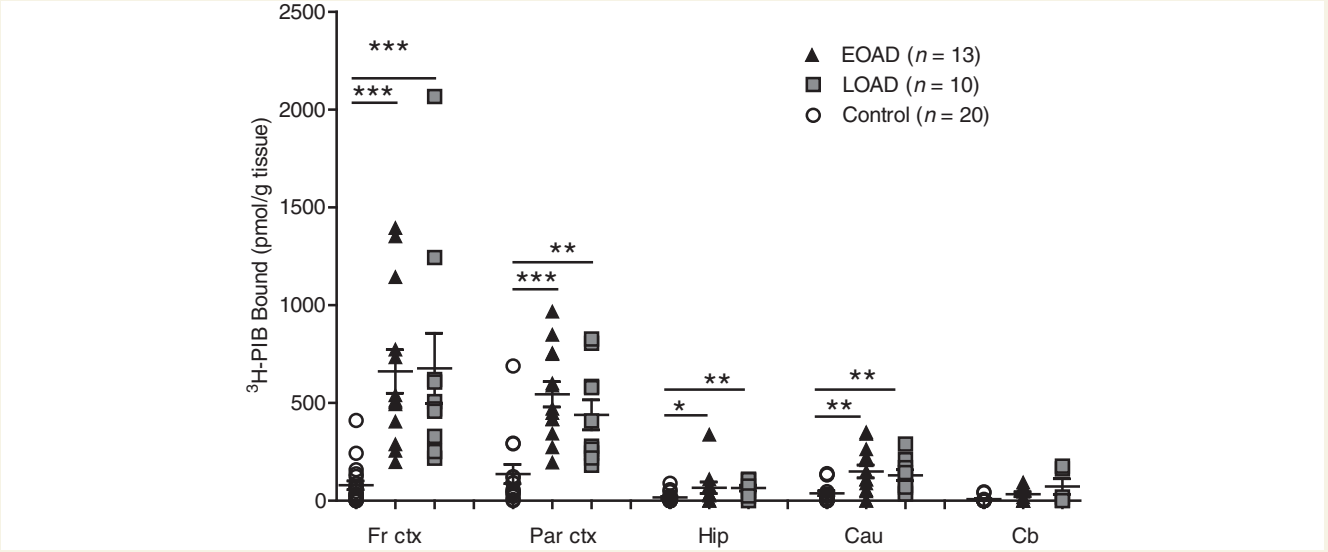

Figure 2 ^{3}H-Pittsburgh compound B (PIB) binding (1 nM) in the frontal cortices (Fr ctx), parietal cortices (Par ctx), hippocampi (Hip), caudate nuclei (Cau) and cerebella (Cb) of brains from patients with early-onset Alzheimer's disease (EOAD; $n = 13$), late-onset Alzheimer's disease (LOAD, $n = 10$) and cognitively normal controls (CTRL; $n = 12$–20). Data are presented as means ± standard error of the mean. Significant differences between early-onset Alzheimer's disease, late-onset Alzheimer's disease and control groups (Mann-Whitney U-test) are indicated by $^*P < 0.05$, $^{**}P < 0.01$ and $^{***}P < 0.001$.

Analysis of the displacement binding results demonstrated the presence of two of three possible binding sites for all the unlabelled amyloid ligands except FDDNP. The affinity for the sites (K_{i1}, K_{i2} or K_{i3}) for these ligands followed the rank order BTA-1 (K_{i1}: 0.2 nM, K_{i2}: 70 nM) > AV-45 (K_{i1}: 1.0 nM, K_{i2}: 65 nM) > AV-1 (K_{i1}: 1.8 nM, K_{i2}: 53 nM) > BF-227 (K_{i1}: 0.3 nM, K_{i3}: 311 nM) (Fig. 3A–D). The proportions of high-affinity binding sites were 88%, 90% and 84% for BTA-1, AV-45 and AV-1, respectively (summarized in Fig. 3A–C). The proportion of high-affinity binding sites for BF-227 was only 17% (Fig. 3D); most of the binding was to the 311 nM affinity site (83%). No K_i value was obtained for FDDNP because ^{3}H-PIB binding was displaced by <50% (Fig. 3E).

Additional autoradiography binding assays were performed in frontal cortex sections from four of the Alzheimer's disease and four of the control brains that were evaluated in the homogenate binding assays. These showed that ^{3}H-PIB binding was completely blocked in the presence of 1 μM BTA-1, AV-45 and AV-1, whereas addition of 1 μM BF-227 or 1 μM FDDNP displaced only 70% and 40% of ^{3}H-PIB binding, respectively (Supplementary Fig. 3).

Discussion

Advances in amyloid PET imaging have already had an impact on the understanding of the time course of Alzheimer's disease pathophysiology (Jack *et al.*, 2013; Nordberg *et al.*, 2010, 2011), as well as the development of biomarkers for early diagnosis, and their use in evaluation of anti-amyloid clinical trials. Recent ongoing debate on amyloid PET imaging has raised questions with regard to the binding properties of different amyloid ligands, their sensitivity and their specificity in reflecting amyloid-β pathology in the Alzheimer's disease brain (Moghbel *et al.*, 2012; Villemagne *et al.*, 2012*a*). This study provides detailed characterization of PIB binding in Alzheimer's disease and normal control post-mortem brain tissue, as well as a comparison of current available amyloid ligands.

The study demonstrated a regional distribution of ^{3}H-PIB binding in the rank order frontal cortex, parietal cortex, caudate nucleus and hippocampus, which is consistent with *in vivo* ^{11}C-PIB PET studies in patients with Alzheimer's disease (Klunk *et al.*, 2004; Mintun *et al.*, 2006; Kemppainen *et al.*, 2006; Rowe *et al.*, 2010; Nordberg *et al.*, 2013). This was also our rationale for focusing on one region as the frontal cortex with high amyloid and hippocampus with low amyloid load in the characterization of ^{3}H-PIB binding in the brain.

We demonstrated the presence of both high-and low-affinity binding sites in the frontal cortex and hippocampus in patients with Alzheimer's disease, and report the presence of a low-affinity site in the cognitively normal control subjects. We also demonstrated that PIB, AV-45 and AV-1 share a common high-affinity binding site with amyloid-β in Alzheimer's disease brain, whereas BF-227 shows lower affinity, and FDDNP has a different binding profile.

The observation of two ^{3}H-PIB binding sites in Alzheimer's disease frontal cortex in this study is in agreement with an earlier report by Klunk *et al.* (2005). To the best of our knowledge, our study is the first to identify the presence of both high- and low-affinity PIB binding sites in the Alzheimer's disease hippocampus. We measured a 30-fold difference in affinity between the two binding sites in both the frontal cortex and the hippocampus, but no difference in affinity for the two sites between these two regions. The proportion of high-affinity to low-affinity sites was

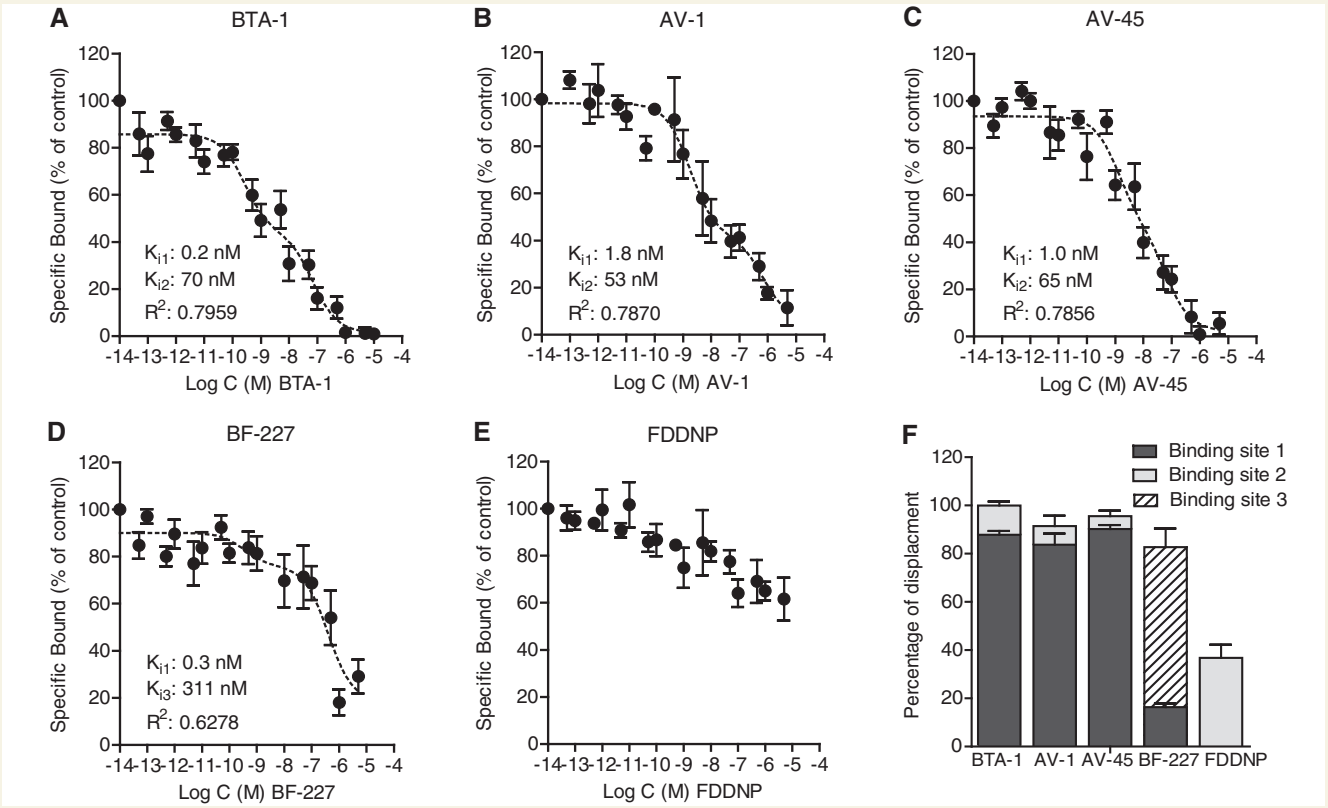

Figure 3 Displacement of ^{3}H-Pittsburgh compound B (PIB) binding by BTA-1, AV-1, AV-45, BF-227 and FDDNP. Competitive binding with ^{3}H-PIB (1 nM) and BTA-1, AV-1 and AV-45 indicated two analogous binding sites (high- and low-affinity; K_{i1} and K_{i2}; **A–C**), whereas a different pattern was detected with BF-227 (K_{i3}; **D**) and FDDNP (K_{i2}; **E**) in the frontal cortices of brains from patients with Alzheimer's disease (AD; $n = 5$). (**F**) Summary of the percentage of displacement of ^{3}H-PIB from binding sites 1, 2 and 3 by the tested unlabelled ligands in the frontal cortices of brains from patients with Alzheimer's disease. Affinity constant (K_i) and percentage displacement values were determined by non-linear regression using GraphPrism. Data are presented as means ± standard error of the mean.

6:1 in the frontal cortex and 3:1 in the hippocampus, with the difference mainly attributable to a greater number of high-affinity binding sites in the frontal cortex than in the hippocampus. The greater difference in amyloid-β_{40} and amyloid-β_{42} ELISA levels between the frontal cortex and hippocampus compared to the ^{3}H-PIB binding in the same brain regions might reflect that ^{3}H-PIB binds solely to fibrillar amyloid-β.

No high-affinity ^{3}H-PIB binding sites were detected in the frontal cortices of the controls, with the exception of one 87-year-old. This observation might have relevance for *in vivo* PET studies with ^{11}C-PIB (Mintun *et al*., 2006; Aizenstein *et al*., 2008; Morris *et al*., 2010; Rowe *et al*., 2010; Sojkova *et al*., 2011), ^{18}F-florbetapir (Rodrigue *et al*., 2012), ^{18}F-florbetaben (Barthel *et al*., 2011) and ^{18}F-flutemetamol (Vandenberghe *et al*., 2010), in which a small proportion of cognitively normal control subjects have shown clear evidence of amyloid tracer retention in the brain. This could be attributed to the time course of amyloid accumulation, as it has been observed that the proportion of cognitively normal control subjects demonstrating high amyloid levels in the brain increases with age, and could have implications for anti-amyloid-β clinical trials in cognitively normal adults (Selkoe, 2012).

Because *in vivo* PET imaging is performed at nanomolar tracer concentrations, low-affinity PIB binding sites cannot be visualized by this method and studies using other techniques are warranted for further detection and characterization of these low-affinity binding sites in the human brain. The presence of low-affinity binding sites could be of mechanistic importance for aggregation processes involving seeding and the progressive development of amyloid-β pathology in the brain, including the occurrence of other smaller forms of amyloid-β such as oligomer assemblies.

In vitro binding studies in fresh tissue brain homogenates have higher sensitivity to detect multiple binding sites than *in vivo* studies since a much broader range of concentrations of both labelled amyloid radiotracer as well a wider concentration range of competing substances can be used in displacement studies. *In vitro* binding studies thus allow detection of binding types with different properties. As the concentration range is broader, high, intermediate and low affinity binding sites can be detected. The *in vivo* PET technique uses amyloid tracer concentrations in a much narrow concentrations range (1–10 nM) and due to risk of toxicity reactions displacement with increasing higher concentrations of unlabelled amyloid tracers have not been able to be performed. Thus so far no saturation studies demonstrating saturation of labelled amyloid binding sites by unlabelled compounds have been able to be performed by PET for any amyloid tracer in humans with the exception of the *in vivo* displacement performed

using non-steroidal anti-inflammatory drugs and ^{18}F-FDDNP (Agdeppa *et al*., 2003).

In the present study the competition assays in tissue homogenates were performed in frontal cortical tissue since frontal cortex shows high ^{3}H-PIB binding, which allows competing reduction in the binding with different agents. The hippocampus was not included in these experiments because the ^{3}H-binding in this brain region opposite to the frontal cortex is low and it is technically much more difficult to obtain reliable displacement values due to larger variation in displacement data.

In vitro binding studies with thioflavin-derived compounds and synthetic amyloid-β polymers have reported that these ligands bind to three classes of binding sites on the amyloid-β fibrils (Lockhart *et al*., 2005; Ye *et al*., 2005). This included binding with very high affinity ($K_d \approx$ low nM) to a low-capacity site (BS3), as well as binding ($K_d \approx 100$ nM) to either one of two additional adjacent or partially overlapping high-capacity binding sites (BS1, BS2) on the amyloid-β_{1-40} polymer (Lockhart *et al*., 2005; Ye *et al*., 2005).

Based on the saturation and displacement assay results in our study, we propose a multiple binding site model (binding sites 1, 2 and 3) for the tested amyloid ligands, as illustrated in Fig. 5F. Competition studies with ^{3}H-PIB revealed that AV-1, AV-45 and BTA-1 bound mainly to the high-affinity (~1 nM) PIB binding site (binding site 1). This is in agreement with earlier saturation binding studies on individual ligands in human brain tissues (Klunk *et al*., 2003; Zhang *et al*., 2005; Choi *et al*., 2009; Kung *et al*., 2010; Fodero-Tavoletti *et al*., 2012). Furthermore, these amyloid ligands also displaced ^{3}H-PIB from the low-affinity binding site 2 ($K_i < 100$ nM).

From PET imaging studies in patients with Alzheimer's disease it is known that ^{11}C-BF-227 is less extensively retained in the cortex in patients with Alzheimer's disease than ^{11}C-PIB (Kudo *et al*., 2007; Furukawa *et al*., 2010; Shao *et al*., 2010). These observations corroborate our finding that BF-227 binding was only 16% to the high-affinity binding site 1, whereas PIB binding to this site was >80%. Instead, a higher proportion of BF-227 binding was with a different low-affinity site from binding sites 1 and 2 (K_{i3} 311 nM; binding site 3) (Fig. 3F).

The displacement of only 40% of ^{3}H-PIB binding by FDDNP suggests that this ligand has a binding profile that differs from that of the other amyloid ligands (Agdeppa *et al*., 2001; Thompson *et al*., 2009). In earlier studies, FDDNP was reported to bind to neurofibrillary tangles in addition to amyloid-β plaques, and it has been suggested that it interacts with the binding of non-steroidal anti-inflammatory drugs (Agdeppa *et al*., 2001; Thompson *et al*., 2009; Petric *et al*., 2012) and also that it binds to a different site on the amyloid-β fibrils from those of PIB (Raman *et al*., 2009; Kung *et al*., 2010; Wu *et al*., 2011). Moreover, a different regional distribution pattern and lower signal range has been observed *in vivo* with ^{18}F-FDDNP compared with ^{11}C-PIB (Shoghi-Jadid *et al*., 2002; Shin *et al*., 2008; Tolboom *et al*., 2009).

One limitation of our study is that only radiolabelled PIB was used in the comparative studies of binding with other amyloid ligands. There is a possibility that, if they had been radiolabelled, these amyloid ligands may have enabled the detection of additional binding sites on amyloid-β fibrils that were not readily recognized by ^{3}H-PIB, and could thus have shown different binding profiles. Additional studies in brain tissue homogenates from carriers of autosomal dominant Alzheimer's disease may most probably provide further insight into difference in amyloid binding sites pattern. In the present study the frontal cortex was chosen as region with high amyloid load. For further studies precuneus would be of great interest with its early high binding of amyloid tracers in course of disease and its correlation with cognitive function in normal subjects (Rosenberg *et al*., 2013).

It will be important in future studies to consider the elucidation of possible binding interactions, other than those on amyloid-β fibrils, between amyloid ligands and other endogenous proteins or receptors. In support of this suggestion, we have recently reported a relationship between high-affinity PIB binding sites and α7 nicotinic receptors in post-mortem Alzheimer's disease brain studies (Lilja *et al*., 2011; Ni *et al*., 2013). Interactions such as these may be intrinsically linked to the neurodegenerative changes in the Alzheimer's disease brain and could necessitate the development of better imaging agents in the future to further advance our understanding of the disease at the molecular level.

In summary, this study indicates the presence of multiple PIB binding sites (high- and low-affinity) in Alzheimer's disease and control brains with confirmed amyloid pathology. From competition studies we propose a multiple site model where PIB, AV-45 (florbetapir) and AV-1 (florbetaben) share similar binding to a nanomolar high affinity site (site 1) and that these amyloid ligands can be used in a comparable and reliable manner to assess brain amyloid density. A somewhat different binding pattern is observed for BF-227 and FDDNP with preference for sites 3 and 2, respectively. Detailed studies of binding characteristics for amyloid PET tracers may provide valuable information for a further understanding of Alzheimer's disease pathology.

Acknowledgements

The authors thank Professor Nobuyuki Okamura (Tohoku University, Sendai, Japan) for the kind gift of BF-227, Professor Jorge R. Barrio (UCLA, CA, USA) for the kind gift of FDDNP, and Dr Ian M. Newington (GE Healthcare, Amersham, UK) for the kind gift of AV-1 and AV-45. We also thank Dr Larysa Voytenko (Karolinska Institutet) and Dr Inger Nennesmo (Karolinska University Hospital Huddinge) for their help with the neuropathological immunohistochemical staining.

Funding

This work was supported by grants from the Swedish Research Council (project 05817), the Karolinska Institutet Strategic Neuroscience programme, the Stockholm County Council-Karolinska Institutet regional agreement on medical training and clinical research (ALF grant), Swedish Brain Power, the Swedish Brain Foundation, the Alzheimer Foundation in Sweden, the Dementia Association, EU FW7 large scale integrating project INMiND (http://www.uni-muenster. de/InMind), the Foundation

for Old Servants, Karolinska Institutet's Foundation for Aging Research, Magnus Bergvall's Foundation, the Olle Engkvist Byggmästare Foundation, Gun and Bertil Stohne's Foundation, the Lars Hierta Memorial Foundation, Sigurd and Elsa Golje's Foundation and Ragnhild and Einar Lundström's Memorial Foundation.

Supplementary material

Supplementary material is available at *Brain* online.

References

Agdeppa ED, Kepe V, Liu J, Flores-Torres S, Satyamurthy N, Petric A, et al. Binding characteristics of radiofluorinated 6-dialkylamino-2-naphthylethylidene derivatives as positron emission tomography imaging probes for beta-amyloid plaques in Alzheimer's disease. J Neurosci 2001; 21: RC189.

Agdeppa ED, Kepe V, Liu J, Small GW, Huang SC, Petric A, et al. 2-Dialkylamino-6-acylmalononitrile substituted naphthalenes (DDNP analogs): novel diagnostic and therapeutic tools in Alzheimer's disease. Mol Imaging Biol 2003; 5: 404–17.

Aizenstein HJ, Nebes RD, Saxton JA, Price JC, Mathis CA, Tsopelas ND, et al. Frequent amyloid deposition without significant cognitive impairment among the elderly. Arch Neurol 2008; 65: 1509–17.

Barthel H, Gertz HJ, Dresel S, Peters O, Bartenstein P, Buerger K, et al. Cerebral amyloid-beta PET with florbetaben (18F) in patients with Alzheimer's disease and healthy controls: a multicentre phase 2 diagnostic study. Lancet Neurol 2011; 10: 424–35.

Bennett DA, Schneider JA, Arvanitakis Z, Kelly JF, Aggarwal NT, Shah RC, et al. Neuropathology of older persons without cognitive impairment from two community-based studies. Neurology 2006; 66: 1837–44.

Choi SR, Golding G, Zhuang Z, Zhang W, Lim N, Hefti F, et al. Preclinical properties of 18F-AV-45: a PET agent for Abeta plaques in the brain. J Nucl Med 2009; 50: 1887–94.

Clark CM, Schneider JA, Bedell BJ, Beach TG, Bilker WB, Mintun MA, et al. Use of florbetapir-PET for imaging beta-amyloid pathology. JAMA 2011; 305: 275–83.

Clark CM, Pontecorvo MJ, Beach TG, Bedell BJ, Coleman RE, Doraiswamy PM, et al. Cerebral PET with florbetapir compared with neuropathology at autopsy for detection of neuritic amyloid-beta plaques: a prospective cohort study. Lancet Neurol 2012; 11: 669–78.

Cselenyi Z, Jonhagen ME, Forsberg A, Halldin C, Julin P, Schou M, et al. Clinical validation of 18F-AZD4694, an amyloid-beta-specific PET radioligand. J Nucl Med 2012; 53: 415–24.

Driscoll I, Troncoso JC, Rudow G, Sojkova J, Pletnikova O, Zhou Y, et al. Correspondence between in vivo (11)C-PiB-PET amyloid imaging and postmortem, region-matched assessment of plaques. Acta Neuropathol 2012; 124: 823–31.

Dubois B, Feldman HH, Jacova C, Cummings JL, Dekosky ST, Barberger-Gateau P, et al. Revising the definition of Alzheimer's disease: a new lexicon. Lancet Neurol 2010; 9: 1118–27.

Engler H, Forsberg A, Almkvist O, Blomquist G, Larsson E, Savitcheva I, et al. Two-year follow-up of amyloid deposition in patients with Alzheimer's disease. Brain 2006; 129 (Pt 11): 2856–66.

Fodero-Tavoletti MT, Brockschnieder D, Villemagne VL, Martin L, Connor AR, Thiele A, et al. In vitro characterization of [(18)F]-florbetaben, an Abeta imaging radiotracer. Nucl Med Biol 2012; 39: 1042–1048.

Forsberg A, Engler H, Almkvist O, Blomquist G, Hagman G, Wall A, et al. PET imaging of amyloid deposition in patients with mild cognitive impairment. Neurobiol Aging 2008; 29: 1456–65.

Furukawa K, Okamura N, Tashiro M, Waragai M, Furumoto S, Iwata R, et al. Amyloid PET in mild cognitive impairment and Alzheimer's disease with BF-227: comparison to FDG-PET. J Neurol 2010; 257: 721–7.

Harada R, Okamura N, Furumoto S, Tago T, Maruyama M, Higuchi M, et al. Comparison of the binding characteristics of [^{18}F]THK-523 and other amyloid imaging tracers to Alzheimerás disease pathology. Eur J Nucl Med Mol Imaging 2013; 40: 125–32.

Ikonomovic MD, Klunk WE, Abrahamson EE, Mathis CA, Price JC, Tsopelas ND, et al. Post-mortem correlates of in vivo PiB-PET amyloid imaging in a typical case of Alzheimer's disease. Brain 2008; 131 (Pt 6): 1630–45.

Jack CR Jr, Lowe VJ, Weigand SD, Wiste HJ, Senjem ML, Knopman DS, et al. Serial PIB and MRI in normal, mild cognitive impairment and Alzheimer's disease: implications for sequence of pathological events in Alzheimer's disease. Brain 2009; 132 (Pt 5): 1355–65.

Jack CR Jr, Knopman DS, Jagust WJ, Petersen RC, Weiner MW, Aisen PS, et al. Tracking pathophysiological processes in Alzheimer's disease -an updated hypothetical model of dynamic biomarkers. Lancet Neurology 2013; 12: 207–16.

Johnson KA, Minoshima S, Bohnen NI, Donohoe KJ, Foster NL, Herscovitch P, et al. Appropriate use criteria for amyloid PET: a report of the amyloid imaging task force, the society of nuclear medicine and molecular imaging, and the alzheimer's association. J Nucl Med 2013; 54: 476–90.

Kadir A, Marutle A, Gonzalez D, Scholl M, Almkvist O, Mousavi M, et al. Positron emission tomography imaging and clinical progression in relation to molecular pathology in the first Pittsburgh Compound B positron emission tomography patient with Alzheimer's disease. Brain 2011; 134 (Pt 1): 301–17.

Kemppainen NM, Aalto S, Wilson IA, Nagren K, Helin S, Bruck A, et al. Voxel-based analysis of PET amyloid ligand [11C]PIB uptake in Alzheimer disease. Neurology 2006; 67: 1575–80.

Kemppainen NM, Aalto S, Wilson IA, Nagren K, Helin S, Bruck A, et al. PET amyloid ligand [11C]PIB uptake is increased in mild cognitive impairment. Neurology 2007; 68: 1603–6.

Klunk WE, Engler H, Nordberg A, Wang Y, Blomqvist G, Holt DP, et al. Imaging brain amyloid in Alzheimer's disease with Pittsburgh Compound-B. Ann Neurol 2004; 55: 306–19.

Klunk WE, Lopresti BJ, Ikonomovic MD, Lefterov IM, Koldamova RP, Abrahamson EE, et al. Binding of the positron emission tomography tracer Pittsburgh compound-B reflects the amount of amyloid-beta in Alzheimer's disease brain but not in transgenic mouse brain. J Neurosci 2005; 25: 10598–606.

Klunk WE, Wang Y, Huang GF, Debnath ML, Holt DP, Shao L, et al. The binding of 2-(4'-methylaminophenyl)benzothiazole to postmortem brain homogenates is dominated by the amyloid component. J Neurosci 2003; 23: 2086–92.

Kudo Y, Okamura N, Furumoto S, Tashiro M, Furukawa K, Maruyama M, et al. 2-(2-[2-Dimethylaminothiazol-5-yl]ethenyl)-6-(2-[fluoro]ethoxy)benzoxazole: a novel PET agent for in vivo detection of dense amyloid plaques in Alzheimer's disease patients. J Nucl Med 2007; 48: 553–61.

Kung HF, Choi SR, Qu W, Zhang W, Skovronsky D. 18F stilbenes and styrylpyridines for PET imaging of A beta plaques in Alzheimer's disease: a miniperspective. J Med Chem 2010; 53: 933–41.

Landau SM, Breault C, Joshi AD, Pontecorvo M, Mathis CA, Jagust WJ, et al. Amyloid-beta imaging with Pittsburgh compound B and Florbetapir: comparing radiotracers and Quantification Methods. J Nucl Med 2013; 54: 70–7.

Leinonen V, Alafuzoff I, Aalto S, Suotunen T, Savolainen S, Nagren K, et al. Assessment of beta-amyloid in a frontal cortical brain biopsy specimen and by positron emission tomography with carbon 11-labeled Pittsburgh Compound B. Arch Neurol 2008; 65: 1304–9.

Leinonen V, Rinne JO, Virtanen KA, Eskola O, Rummukainen J, Huttunen J, et al. Postitron emission tomography with [(18)F]flumetamol and [(11) C] PIB for in vivo detection cerebral

cortical amyloid in normal pressure hydrocephalus patients. Eur J Neurol 2013, doi: 10.1111/ene.12102.
Lilja AM, Porras O, Storelli E, Nordberg A, Marutle A. Functional interactions of fibrillar and oligomeric amyloid-β with alpha7 nicotinic receptors in Alzheimer's disease. Journal of ALzheimer's disease 2011; 23: 335–47.
Lockhart A, Ye L, Judd DB, Merritt AT, Lowe PN, Morgenstern JL, et al. Evidence for the presence of three distinct binding sites for the thioflavin T class of Alzheimer's disease PET imaging agents on beta-amyloid peptide fibrils. J Biol Chem 2005; 280: 7677–84.
McKhann GM, Knopman DS, Chertkow H, Hyman BT, Jack CR Jr, Kawas CH, et al. The diagnosis of dementia due to Alzheimer's disease: recommendations from the National Institute on Aging-Alzheimer's Association workgroups on diagnostic guidelines for Alzheimer's disease. Alzheimers Dement 2011; 7: 263–9.
Mintun MA, Larossa GN, Sheline YI, Dence CS, Lee SY, Mach RH, et al. [11C]PIB in a nondemented population: potential antecedent marker of Alzheimer disease. Neurology 2006; 67: 446–52.
Moghbel MC, Saboury B, Basu S, Metzler SD, Torigian DA, Langstrom B, et al. Amyloid-beta imaging with PET in Alzheimer's disease: is it feasible with current radiotracers and technologies? Eur J Nucl Med Mol Imaging 2012; 39: 202–8.
Morris JC, Roe CM, Xiong C, Fagan AM, Goate AM, Holtzman DM, et al. APOE predicts amyloid-beta but not tau Alzheimer pathology in cognitively normal aging. Ann Neurol 2010; 67: 122–31.
Nelissen N, Van Laere K, Thurfjell L, et al. Phase I study of the PIB derivative 18F-flutemetamol in healthy volunteers and patients with probable Alzheimer's disease. J Nucl Med 2009; 50: 1251–9.
Ni R, Marutle A, Nordberg A. Modulation of alpha7 nicotinic acetylcholine receptor and fibrillar amyloid-beta interactions in Alzheimer's Disease Brain. J Alzheimers Dis 2013; 33: 841–51.
Nordberg A, Rinne JO, Kadir A, Langstrom B. The use of PET in Alzheimer disease. Nat Rev Neurol 2010; 6: 78–87.
Nordberg A. Molecular imaging in Alzheimer's disease: new perspectives on biomarkers for early diagnosis and drug development. Alzheimers Res Ther 2011; 3: 34.
Nordberg A, Carter SF, Rinne J, Drzezga A, Brooks DJ, Vandenberghe R, et al. A European multicentre PET study of fibrillar amyloid in Alzheimer's disease. Eur J Nucl Med Mol Imaging 2013; 40: 104–14.
Nyberg S, Jonhagen ME, Cselenyi Z, Halldin C, Julin P, Olsson H, et al. Detection of amyloid in Alzheimer's disease with positron emission tomography using [11C]AZD2184. Eur J Nucl Med Mol Imaging 2009; 36: 1859–63.
Petric A, Johnson SA, Pham HV, Li Y, Ceh S, Golobic A, et al. Dicyanovinylnaphthalenes for neuroimaging of amyloids and relationships of electronic structures and geometries to binding affinities. Proc Natl Acad Sci U S A 2012; 109: 16492–7.
Pike KE, Savage G, Villemagne VL, Ng S, Moss SA, Maruff P, et al. Beta-amyloid imaging and memory in non-demented individuals: evidence for preclinical Alzheimer's disease. Brain 2007; 130 (Pt 11): 2837–44.
Price JL, Morris JC. Tangles and plaques in nondemented aging and "preclinical" Alzheimer's disease. Ann Neurol 1999; 45: 358–68.
Raman EP, Takeda T, Klimov DK. Molecular dynamics simulations of Ibuprofen binding to Abeta peptides. Biophys J 2009; 97: 2070–9.
Reiman EM, Jagust WJ. Brain imaging in the study of Alzheimer's disease. Neuroimage 2012; 61: 505–16.
Rodrigue KM, Kennedy KM, Devous MD Sr, Rieck JR, Hebrank AC, Diaz-Arrastia R, et al. beta-Amyloid burden in healthy aging: regional distribution and cognitive consequences. Neurology 2012; 78: 387–95.
Rosenberg PB, Wong DF, Edell SL, Ross JS, Joshi AD, Brasic JR, et al. Cognition and amyloid load in Alzheimer disease imaged with florbetapir F18 (AV-45) positron emission tomography. Am J Ger Psychiatry 2013; 21: 272–8.
Rowe CC, Ackerman U, Browne W, Mulligan R, Pike KL, O'Keefe G, et al. Imaging of amyloid beta in Alzheimer's disease with 18F-BAY94-9172, a novel PET tracer: proof of mechanism. Lancet Neurol 2008; 7: 129–35.
Rowe CC, Ellis KA, Rimajova M, Bourgeat P, Pike KE, Jones G, et al. Amyloid imaging results from the Australian Imaging, Biomarkers and Lifestyle (AIBL) study of aging. Neurobiol Aging 2010; 31: 1275–83.
Rowe CC, Ng S, Ackermann U, Gong SJ, Pike K, Savage G, et al. Imaging beta-amyloid burden in aging and dementia. Neurology 2007; 68: 1718–25.
Rowe CC, Villemagne VL. Brain amyloid imaging. J Nucl Med 2011; 52: 1733–40.
Selkoe DJ. Preventing Alzheimer's disease. Science 2012; 337: 1488–92.
Shao H, Okamura N, Sugi K, Furumoto S, Furukawa K, Tashiro M, et al. Voxel-based analysis of amyloid positron emission tomography probe [C]BF-227 uptake in mild cognitive impairment and alzheimer's disease. Dement Geriatr Cogn Disord 2010; 30: 101–11.
Shin J, Lee SY, Kim SH, Kim YB, Cho SJ. Multitracer PET imaging of amyloid plaques and neurofibrillary tangles in Alzheimer's disease. Neuroimage 2008; 43: 236–44.
Shoghi-Jadid K, Small GW, Agdeppa ED, Kepe V, Ercoli LM, Siddarth P, et al. Localization of neurofibrillary tangles and beta-amyloid plaques in the brains of living patients with Alzheimer disease. Am J Geriatr Psychiatry 2002; 10: 24–35.
Sojkova J, Driscoll I, Iacono D, Zhou Y, Codispoti KE, Kraut MA, et al. *In vivo* fibrillar beta-amyloid detected using [11C]PiB positron emission tomography and neuropathologic assessment in older adults. Arch Neurol 2011; 68: 232–40.
Sperling RA, Aisen PS, Beckett LA, Bennett DA, Craft S, Fagan AM, et al. Toward defining the preclinical stages of Alzheimer's disease: recommendations from the National Institute on Aging-Alzheimer's Association workgroups on diagnostic guidelines for Alzheimer's disease. Alzheimers Dement 2011; 7: 280–92.
Thompson PW, Ye L, Morgenstern JL, Sue L, Beach TG, Judd DJ, et al. Interaction of the amyloid imaging tracer FDDNP with hallmark Alzheimer's disease pathologies. J Neurochem 2009; 109: 623–30.
Tolboom N, Yaqub M, van der Flier WM, Boellaard R, Luurtsema G, Windhorst AD, et al. Detection of Alzheimer pathology in vivo using both 11C-PIB and 18F-FDDNP PET. J Nucl Med 2009; 50: 191–7.
Vandenberghe R, Van Laere K, Ivanoiu A, Salmon E, Bastin C, Triau E, et al. 18F-flutemetamol amyloid imaging in Alzheimer disease and mild cognitive impairment: a phase 2 trial. Ann Neurol 2010; 68: 319–29.
Verhoeff NP, Wilson AA, Takeshita S, Trop L, Hussey D, Singh K, et al. In-vivo imaging of Alzheimer disease beta-amyloid with [11C]SB-13 PET. Am J Geriatr Psychiatry 2004; 12: 584–95.
Villain N, Chetelat G, Grassiot B, Bourgeat P, Jones G, Ellis KA, et al. Regional dynamics of amyloid-beta deposition in healthy elderly, mild cognitive impairment and Alzheimer's disease: a voxelwise PiB-PET longitudinal study. Brain 2012; 135 (Pt 7): 2126–39.
Villemagne VL, Burnham S, Bourgeat P, Brown B, Ellis KA, Salvado O, et al. Australian Imaging Biomarkers and Lifestyle (AIBL) Resarch Group. Amyloid ß deposition, neurodegeration, and cognitive decline in sporadic Alzheimerás disease: a prospective cohort study. Lancet Neurol 2013; 12: 357–67.
Villemagne VL, Klunk WE, Mathis CA, Rowe CC, Brooks DJ, Hyman BT, et al. Abeta Imaging: feasible, pertinent, and vital to progress in Alzheimer's disease. Eur J Nucl Med Mol Imaging 2012a; 39: 209–19.
Villemagne VL, Mulligan RS, Pejoska S, Ong K, Jones G, O'Keefe G, et al. Comparison of 11C-PiB and 18F-florbetaben for Abeta imaging in ageing and Alzheimer's disease. Eur J Nucl Med Mol Imaging 2012b; 39: 983–9.
Villemagne VL, Pike KE, Chetelat G, Ellis KA, Mulligan RS, Bourgeat P, et al. Longitudinal assessment of Abeta and cognition in aging and Alzheimer disease. Ann Neurol 2011; 69: 181–92.
Wolk DA, Grachev ID, Buckley C, Kazi H, Grady MS, Trojanowski JQ, et al. Association between in vivo fluorine 18-labeled flutemetamol amyloid positron emission tomography imaging and in vivo cerebral cortical histopathology. Arch Neurol 2011; 68: 1398–403.
Wolk DA, Zhang Z, Boudhar S, Clark CM, Pontecorvo MJ, Arnold SE. Amyloid imaging in Alzheimer's disease: comparison of florbetapir and

Pittsburgh compound-B positron emission tomography. J Neurol Neurosurg Psychiatry 2012; 83: 923–6.

Wong DF, Rosenberg PB, Zhou Y, Kumar A, Raymont V, Ravert HT, et al. *In vivo* imaging of amyloid deposition in Alzheimer disease using the radioligand 18F-AV-45 (florbetapir [corrected] F 18). J Nucl Med 2010; 51: 913–20.

Wu C, Bowers MT, Shea JE. On the origin of the stronger binding of PIB over thioflavin T to protofibrils of the Alzheimer amyloid-beta peptide: a molecular dynamics study. Biophys J 2011; 100: 1316–24.

Ye L, Morgenstern JL, Gee AD, Hong G, Brown J, Lockhart A. Delineation of positron emission tomography imaging agent binding sites on beta-amyloid peptide fibrils. J Biol Chem 2005; 280: 23599–604.

Zhang W, Oya S, Kung MP, Hou C, Maier DL, Kung HF. F-18 stilbenes as PET imaging agents for detecting beta-amyloid plaques in the brain. J Med Chem 2005; 48: 5980–8.